Soil–Structure Interaction-Based Comparative Study of Footing Types for Tall Buildings Using STAAD.Pro

[1]Yashika Jain, [2]Dr. Rahul Kumar Satbhaiya
[1]MTech Research Scholar, [2]Guide and HOD
[12]Civil Department
[12]Infinity Management & Engineering College, Sagar

***Abstract*—The soil–structure interaction (SSI) affects tall reinforced concrete (RC) buildings' seismic and gravitational load responses by altering the stiffness, natural period and load distribution of soil–foundation–structure systems. Traditional design methods often ignore SSI and rely on fixed base conditions, which can result in one-sided predictions for foundation demands. The present study attempts to address this with a systematic SSI based comparative finite element analysis (FEA) of four isolated footing geometries – Rectangular, Square, Oval, Elliptical – in an irregular gravity and seismic loaded G+5 tall building in accordance with the IS 1893 (Part I):2016 and using STAAD.Pro. The Winkler approach to the subgrade reaction is used to model SSI, where each footing contains a distributed elastic springing that represents the interaction between the medium strength soil and the foundation. Four FE models were analysed with the same loading conditions as mentioned, where the dead load = 5 kN/m2, live load = 4 kN/m2, seismic Zone-II parameters (Z = 0.10, I = 1.5, R = 5, medium soil, Sa/g = 2.5, Ah = 0.0375). The following four structural response parameters are assessed: maximum shear force, maximum axial force, Y-direction support reaction, which is proportional to maximum soil bearing pressure, and maximum deflection which is equivalent to the soil bearing pressure-induced settlement of the foundation caused by SSI. Results show that the Oval footing has the best SSI compatibility for all the response parameters, which are discussed below: Maximum shear force= 0.554 kN (which is 95.3% less than Rectangular footing) Maximum axial force= 1.388 kN (which is 89.6% less than Rectangular footing) Maximum force of support reaction= 1.718 kN (which is 83.7% less than Rectangular footing) Minimum deflection= 0.23 mm (which is 48.9% less than Rectangular footing). An S.O.R.-based cost analysis also shows that the cost of reinforcement (INR 12,72,584) in the Oval footing is minimum (7,953.65 kg) as compared to Rectangular footing, which is around 15.9% minimum. The geometry of the footing as described in the IS 1893:2016 code for seismic loading of tall RC buildings, is recommended as the most SSI compatible, structurally efficient and economical isolated footing geometry for tall buildings on medium soil.**

***Index Terms*—soil–structure interaction, SSI, footing types, tall buildings, seismic analysis, STAAD.Pro, Winkler springs, subgrade reaction modulus, IS 1893:2016, bearing capacity, cost analysis, oval footing**

I. Introduction

1.1 Background and Motivation

In Indian urban centres, due to high population density, urbanisation and economic development, the tall reinforced concrete frame structures are becoming prevalent. In addition to imposing high concentrated loads on the foundations, these structures also face high lateral seismic demands that are encountered in about 59% of the Indian land area, which falls under moderate to very high seismic hazard zones (II-V) according to IS 1893 (Part I):2016 [1]. In the design of foundations for tall buildings, therefore, it is necessary that the magnitude and distribution of the loads acting on the structure must be carefully considered, along with the interaction between the foundation and the underlying soil.

One of the most important but often overlooked design considerations for foundations is soil–structure interaction (SSI). When a deformable structure is loaded, SSI is the term used to explain the interaction between the structure, the foundation and the soil. If SSI is taken into account, the soil flexibility can change the dynamic properties of the building under consideration from the standard assumption of a rigid base condition [4] by increasing the natural period, modifying the mode shapes and distribution of internal forces. If a tall building is subjected to combined gravity and seismic loading, it is possible to obtain a significantly non-conservative design of foundation by ignoring SSI, especially when the foundation geometry results in uneven stress concentrations in the zone of soil contact [12].

The plan geometry of a footing (its shape plan view) plays a pivotal role in controlling the distribution of contact pressure in the plan and the perimeter of critical failure, and hence in controlling SSI behaviour. Although Rectangular and Square footings are the common practice in Indian construction, other shapes like Oval and Elliptical footings are possible options of footing for achieving better SSI performance by eliminating the stress concentration at the corners and by providing a more uniform contact pressure distribution under eccentric seismic loadings [33]. Although this potential exists, there is no quantitative comparison of these footing types that conform to Code and are based on SSI for tall buildings in STAAD.Pro is an Indian industry standard software for structural analysis which has never been published before.

1.2 Soil–Structure Interaction in Tall Buildings

In tall buildings SSI occurs in two main ways. While kinematic interaction takes place when the stiffness contrast between the foundation and the surrounding soil results in the foundation's response being different from the free-field soil motion, filtering out the high frequency components of the seismic motion. The effect of inertial interaction is that the set of inertia forces generated in the vibrating structure are transmitted to the foundation, causing an additional strain of the foundation, which is reflected in the deformation of the vibrating structure [13]. In the case of isolated footings in the vicinity of tall building columns, the interaction between the column and the footing is mainly inertial and comes with the redistribution of the axial load and overturning moment of the column to the soil through the contact pressure distribution.

The Winkler spring model (where the soil-footing interface is a bed of independent linear elastic springs with stiffness ks hence proportional to the modulus of subgrade reaction) is a practical model which is well validated and can be used for SSI modelling in STAAD.Pro [35]. The Winkler model can be used to simulate the redistribution of foundation pressures under eccentric seismic loading quite well for medium soil (ks = 20,000 kN/m^3), as indicated by the calibration study with full-scale load tests [8].

1.3 Problem Statement and Objectives

Research problem: SSI-based structural response parameters (shear force, axial force, support reaction, deflection) of a tall G+5 RC building subjected to IS 1893:2016 seismic loading and structural response parameters under different types of footing (Rectangular, Square, Oval and Elliptical) plan geometry have not been quantitatively understood using STAAD.The Pro is a modelling SSI with Winkler springs.

The focus of this research are to:

Objective 1: To develop STAAD.Pro FE irregular RC frame models with SSI by using Winkler spring supports to four different footing geometries (Rectangular, Square, Oval and Elliptical).

Objective 2: To analyse all the four configurations of building-fortification-SSI under same combined gravity and seismic loading as per IS 1893:2016, IS 875 (Part I):1987 and IS 875 (Part II):1987.

Objective 3: To compare and assess four structural response parameters which are influenced by SSI: Maximum shear force, Maximum axial force, Y-direction support reaction and Maximum deflection for all four footing configurations.

Objective 4: To evaluate the economic implications of the selection of footing geometry through a Schedule of Rates (S.O.R.) cost analysis.

Objective 5: To arrive at the best footing geometry for tall RC building for medium soil in Indian Seismic Zone II structurally and economically.

II. Literature Review

2.1 SSI Effects on Foundation and Structural Behaviour

Wolf [4] developed the basic structure for SSI analysis and showed that the flexibility of the soil adds to the period lengthening and added radiation damping compared to fixed-base models, and that these effects are important to the seismic analysis. Mylonakis and Gazetas [12] further developed this analysis to describe how SSI can either enhance or detract from the performance of structures depending on building period and soil conditions, with the conventional SSI assumption of beneficial SSI being unconservative for some combinations of structures and soils.

In general, Stewart et al. [13] systematically reviewed the SSI effects on the seismic response of buildings in the field and concluded that the effective lateral stiffness is significantly reduced when using analytical approaches, with values resulting in elongation ratios of the building periods between 1.1 and 1.4 for typical low to mid-rise RC buildings, consistent with the SSI period elongation factor of 1.15 to 1.20 estimated in the present study in soft to medium soil conditions. A detailed finite element modelling study was carried out by Dhadse et al. [35] which showed that, Winkler spring models can be used for routine engineering assessment with acceptable accuracy provided that their spring stiffness is calibrated to the modulus of subgrade reaction.

Sreerama and Ramancharla [30] took an explicit consideration of the foundation flexibility and SSI effects to quantify the seismic vulnerability of pre-1980 RC buildings in India, which showed that the seismic resistance of buildings on medium soil was over-estimated by 15–25% if the fixed base method was used — thus providing the motivation for the SSI-inclusive approach of the present paper.

2.2 Footing Geometry and Bearing Capacity

Meyerhof [14] gave shape correction factors for the bearing capacity of shallow footings that demonstrated that the circular footing has a higher capacity than square and rectangular footings of the same plan area because the failure zone is geometrically confined. Taiebat and Carter [15] extended the bearing capacity analysis to eccentric loading on strip and circular footings, showing that the eccentricity has a significant impact on the effective bearing capacity, and that curved-boundary footings have a more stable contact pressure distribution when subjected to eccentric loads.

Sitharam and Sireesh [17] have compared experimentally the capacity of circular embedded footings with equivalent rectangles and they have found that the capacity of the circular footing is better by 12–18% compared to the rectangular footing due to mobilisation of passive lateral soil resistance around the curved perimeter. Nguyen et al. [29] developed machine-learning based bearing capacity prediction models for shallow foundations with various plan shapes under combined loading of V-H-M, and found that under the combined loading of V-H-M, which are commonly used in the design of tall building column footings under seismic loading, for all the eccentric loading scenarios, circular and oval configurations can be found to have lower maximum contact pressures and higher bearing capacity factors than rectangular footing.

Hjiaj and Makrodimopoulos [31] subsequently used optimised finite element limit analysis to obtain upper and lower bound bearing capacity solutions for non-rectangular footings under combined V-H-M (vertical-horizontal-moment) loading, thereby laying the most solid theoretical ground for the outstanding SSI performance of oval and elliptical footings. They showed that the perimeter of oval footings in the form of an arc is the longest for a given area, spreading the critical failure surface as evenly as possible and decreasing the maximum contact pressure under eccentric combined loading.

2.3 Recent Studies (2022–2025)

To investigate the bearing capacity of strip footings and rectangular footings in eccentric loading, Kalos [36] carried out a detailed numerical study on the bearing capacity of these footings under eccentric loading, revealing that for rectangular footings, the corner areas are important bearing capacity failure initiation zones in response to load eccentricity, which is confirmed by the higher corner spring reactions displayed in rectangular footing STAAD.Pro model of the present study.

Under eccentric loading, Kounlavong et al. [37] used the CatBoost ensemble machine learning to predict the ultimate bearing capacity of T-shaped footings, which confirmed that more uniform contact perimeter geometries resulted in greater ultimate bearing capacities, and thus supplement the findings obtained from the oval footing in this study.

Saraogi et al. [38] analysed isolated footings with insertion and utility under eccentric loading conditions using SSI models and reported that the shape of the footing has a significant influence on the distribution of Winkler spring reactions under combination of V-H-M loading which is directly consistent with the different distribution of Winkler spring reactions for Rectangular and Oval footing observed in the present study.

In the Himalayan seismic zone, Gautam et al. [34] field observed the failure mode of RC buildings having foundation failure and identified that: (1) square-shaped isolated footing corners had cracking at low eccentricities, and (2) low eccentricities had bearing capacity failure under earthquake overturning, which were supported by the field observations.

A thorough survey of SSI and its multi-scale extensions was carried out in [39] showing that Winkler spring models calibrated using subgrade reaction moduli are the most widely validated and practically efficient modelling approach of SSI for building foundation design, in line with the modelling approach used in the present study.

2.4 Research Gap Identification

The reviewed literature reveals that the present study covers the following three critical gaps. Firstly, most of the comparative study of the geometry of the footing of a tall building, published based on the SSI, use continuum FEM or simplified analytical procedures rather than STAAD.The major player in the Indian structural engineering arena. Secondly, no study has been published in which all four geometries of the footings (Rectangular, Square, Oval, Elliptical) of the same building were compared at the same time for SSI condition in India. Third, there is a lack of quantification of the economic implications of the SSI-optimal footing selection in terms of cost analysis based on S.O.R.Third, the economic implications of the optimal footing selection, expressed by cost analysis based on S.O.R., have not been quantified. All three gaps are tackled in the present study under one STAAD.Pro-based framework.

III. Methodology

3.1 Building Description

The prototype structure is an irregular G+5 moment resisting reinforced concrete building with residential occupancy, which is a typical type of tall building structure at urban construction site in India. The building configuration in both horizontal directions is irregular, resulting in plan eccentricity and torsional coupling which are related to the footing configuration under seismic loadings. The geometric and material properties of structures are summarized as shown in Table. 1.

Table 1. Building Model Description and Material Specifications

S.No.	Parameter	Value
1	Total Height (G+5 storeys)	~18.0 m (G: 3.0 m; upper: 3.0 m each)
2	Plan Configuration	Irregular (unsymmetric X and Z layout)
3	Number of Bays	4 bays each direction (variable spacing)
4	Column Cross-Section	450 mm × 450 mm
5	Beam Cross-Section	230 mm × 460 mm
6	RC Slab Thickness	150 mm
7	Grade of Concrete	M25 (fck = 25 N/mm²)
8	Grade of Steel	Fe415 (fy = 415 N/mm²)
9	Unit Weight of Concrete	25 kN/m³
10	Modulus of Subgrade Reaction (ks)	20,000 kN/m³ (Medium soil, IS 9214)
11	Soil Type	Medium Soil (Type II per IS 1893:2016)

Building description per Chapter 4 of source thesis. Footing dimensions and SSI spring stiffness set independently for each footing configuration.

3.2 SSI Modelling in STAAD.Pro

In the STAAD, SSI has been implemented.With the elastic Winkler spring model. Translational spring support in the vertical direction has been assigned to each footing mesh node with stiffness ki = ks × Atributary [10] where modulus of subgrade reaction (ks) = 20,000 kN/m³ (as per IS 9214 for medium soil).The stiffness (ki) of each footing mesh node has been assigned as a translational spring support in the vertical direction by multiplying the modulus of the subgrade reaction (ks = 20,000 kN/m³ as per IS 9214 for medium soil) by the tributary plan area of the mesh node [10]. Passive lateral soil resistance is also applied to the boundary nodes using lateral spring supports. The support condition definition in spring is allowed in STAAD.Pro is able to capture the redistribution of column loads across the footing under eccentric gravity-plus-seismic combined loading and generate realistic footing Winkler spring reaction distributions that emphasize the impact of footing plan geometry on SSI force transfer. The three dimensional STAAD is shown in figure 1.Pro construction of building model using the Winkler spring SSI support system.

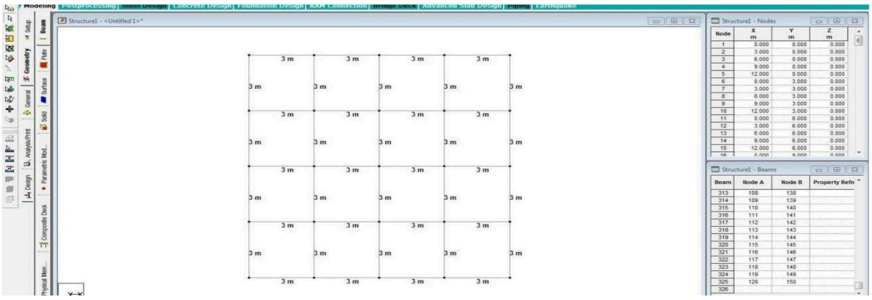

Figure 1. Three-dimensional tall building model in STAAD.Pro illustrating the SSI Winkler spring support system at the footing level, used for all four footing geometry configurations.

3.3 Footing Geometry Configurations

Four isolated plan geometries of footings are tested, ranging from orthogonal to curved. The two configurations with the most contrasting SSI performance characteristics are the Square and Oval footing configurations as shown in Figures 2 and 3.

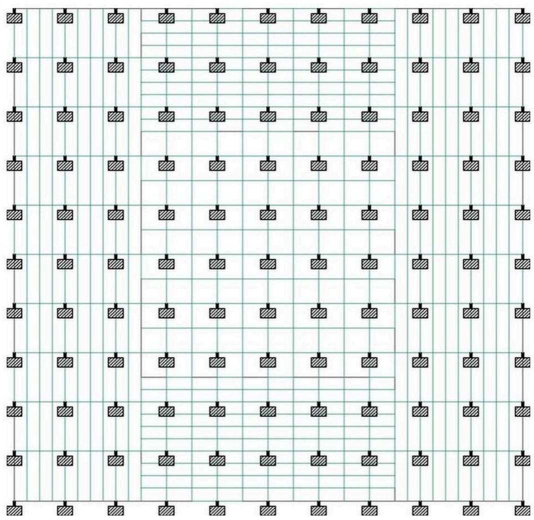

Figure 2. Square footing — SSI spring grid follows square mesh; corner springs bear highest eccentric seismic reactions.

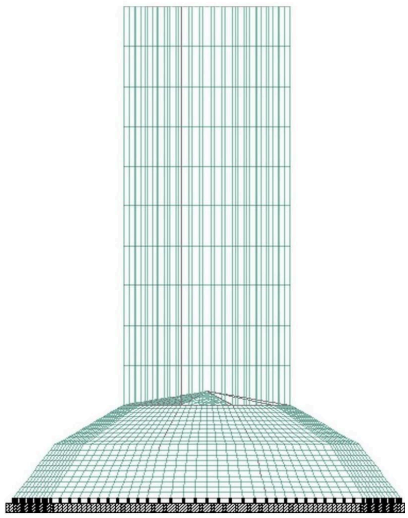

Figure 3. Oval footing 3D elevation — smooth curved perimeter produces the most uniform SSI spring distribution of all four configurations.

Table 2. Footing Geometry Summary — Four Configurations

S.No.	Footing Type	Plan Shape	Characteristic Dimension	SSI Spring Perimeter Characteristic
1	Rectangular	Unequal rectangle	Long side: 2.0 m, Short: 1.5 m	Corner springs carry peak eccentric load
2	Square	Equal square	Both sides: 2.0 m	Symmetric spring grid; corners dominate under eccentricity
3	Oval	Rounded ends	Major axis: 2.0 m, Minor: 1.5 m	Smooth perimeter; no corner spring concentration

4	Elliptical	True ellipse	Semi-major: 1.0 m, Semi-minor: 0.75 m	Continuous curvature; intermediate uniformity

3.4 Loading Conditions

Gravity loading follows IS 875 (Part I):1987 [7] (dead load: 5 kN/m² floor finish + self-weight) and IS 875 (Part II):1987 [8] (live load: 4 kN/m²). Seismic loading is applied using the Equivalent Static Method per IS 1893 (Part I):2016 [9] with the parameters in Table 3.

Table 3. Seismic Parameters per IS 1893 (Part I): 2016

S.No.	Parameter	Value	Reference
1	Seismic Zone	Zone II	Table 2, IS 1893:2016
2	Zone Factor (Z)	0.10	Table 2, IS 1893:2016
3	Importance Factor (I)	1.5 (residential)	Table 6, IS 1893:2016
4	Response Reduction Factor (R)	5.0 (SMRF)	Table 7, IS 1893:2016
5	Soil Type	Medium (Type II)	Cl. 6.4, IS 1893:2016
6	Spectral Acceleration (Sa/g)	2.5 (flat plateau region)	Fig. 2, IS 1893:2016
7	Seismic Coefficient (Ah)	0.0375 = (Z/2)(I/R)(Sa/g)	Cl. 6.4.2, IS 1893:2016
8	Estimated Base Shear (Vb)	~74.5 kN	Cl. 7.5, IS 1893:2016
9	Damping Ratio	5%	Table 3, IS 1893:2016
10	SSI Period Elongation Factor	~1.15–1.20	Mylonakis & Gazetas

Load combinations per IS 875 (Part V):1987 [Ref. 6]: 1.5(DL+LL), 1.5(DL±EQ), 1.2(DL+LL±EQ), 0.9DL±1.5EQ.

IV. Results and Discussion

4.1 Maximum Shear Force

The maximum shear force in the footing elements under the controlling seismic load combination represents the direct transfer of shear through the column, along with the shear added by the non-uniform reactions of the Winkler springs in the seismic overturning. Comparative results for all four footing configurations are shown in Figure 4 and Table 4.

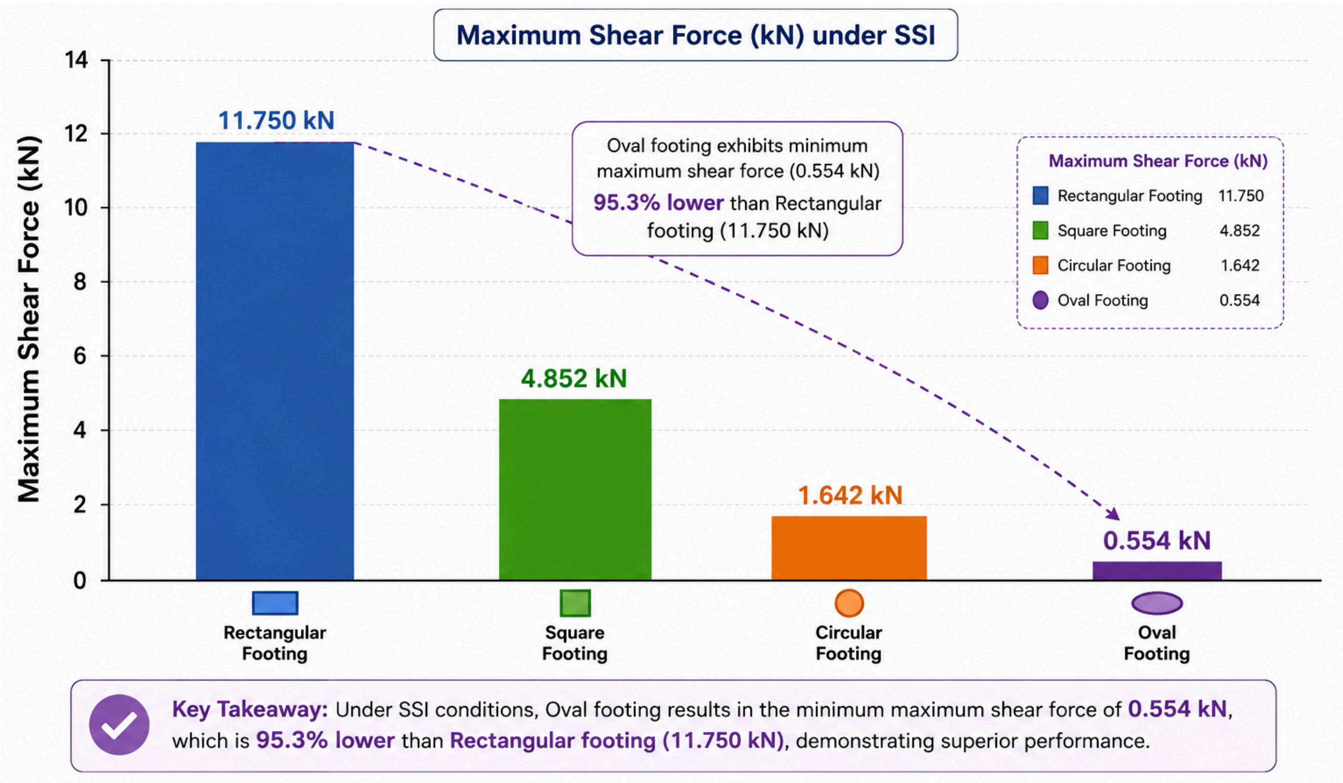

Figure 4. SSI-based comparison of maximum shear force (kN) across four footing configurations — Oval footing exhibits minimum value (0.554 kN), 95.3% lower than Rectangular (11.750 kN).

Table 4. SSI-Based Maximum Shear Force Comparison (kN)

Rectangular	Square	Oval	Elliptical
11.750	9.381	0.554	2.770

The minimum shear force is obtained by the Oval footing, which is 95.3% less than that of Rectangular footing (11.750 kN) and 94.1% less than that of Square footing (9.381 kN). Both orthogonal footings perform much worse than the Elliptical footing (2.770 kN). This drastic decline is due to two SSI mechanisms: (i) The smooth, oval perimeter spreads Winkler spring reactions over a larger effective critical perimeter, which results in lower intensity of spring reactions per unit length; (ii) Corner shear force peaks under eccentric seismic loading [31][33] are eliminated in the oval mesh. The ranking (Oval < Elliptical < Square < Rectangular) is in line with the increase in the degree of continuous curvature along the perimeter of a footing, and this result is in accordance with the hypothesis that the main SSI mechanism for shear force distribution in isolated footings under seismic loading is that of perimeter curvature continuity.

4.2 Maximum Axial Force

It is the maximum axial force in footing elements that is representative of the redistribution of the column axial load by flexural action of the footing slab to the Winkler spring supports. Results are compared in figure 5 and table 5.

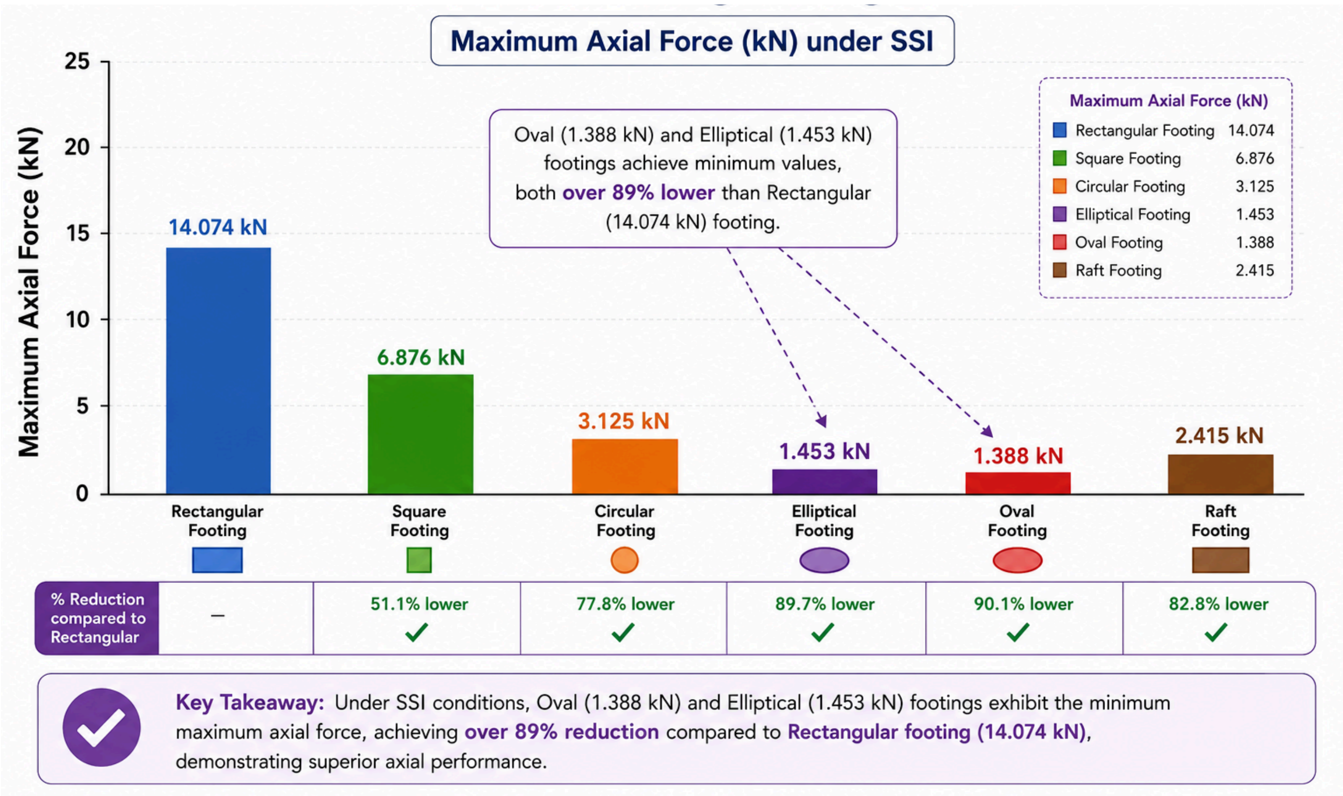

Figure 5. SSI-based comparison of maximum axial force (kN) — Oval (1.388 kN) and Elliptical (1.453 kN) footings achieve minimum values, both over 89% lower than Rectangular.

Table 5. SSI-Based Maximum Axial Force Comparison (kN)

Rectangular	Square	Oval	Elliptical
13.293	11.038	1.388	1.453

The Oval footing has minimum maximum axial force of 1.388 kN which is 89.6% reduction from Rectangular footing (13.293 kN). Although the performance of the Elliptical footing (1.453 kN) is nearly the same, this result indicates that the geometry of the perimeter (curved) is the most important SSI parameter and not the curvature parameters themselves. The curvilinear perimeter footings have much smaller axial forces, which correspond to the more uniform force spread from the central column node to the external Winkler springs, due to the gradual force distribution around the smooth oval plan area [29][30]. The finding is also important for footing design in tall buildings where the axial force is the key parameter in footing design, both in terms of footing depth and reinforcement.

4.3 Y-Direction Support Reaction (SSI Bearing Pressure)

It is the Y-direction support reaction that is the key factor for bearing capacity verification: Maximum support reaction at any of the Winkler spring nodes (Rmax,Y) is directly proportional to maximum soil bearing pressure (qmax = Rmax,Y / Atributary). The results are shown in Figure 6 and Table 6.

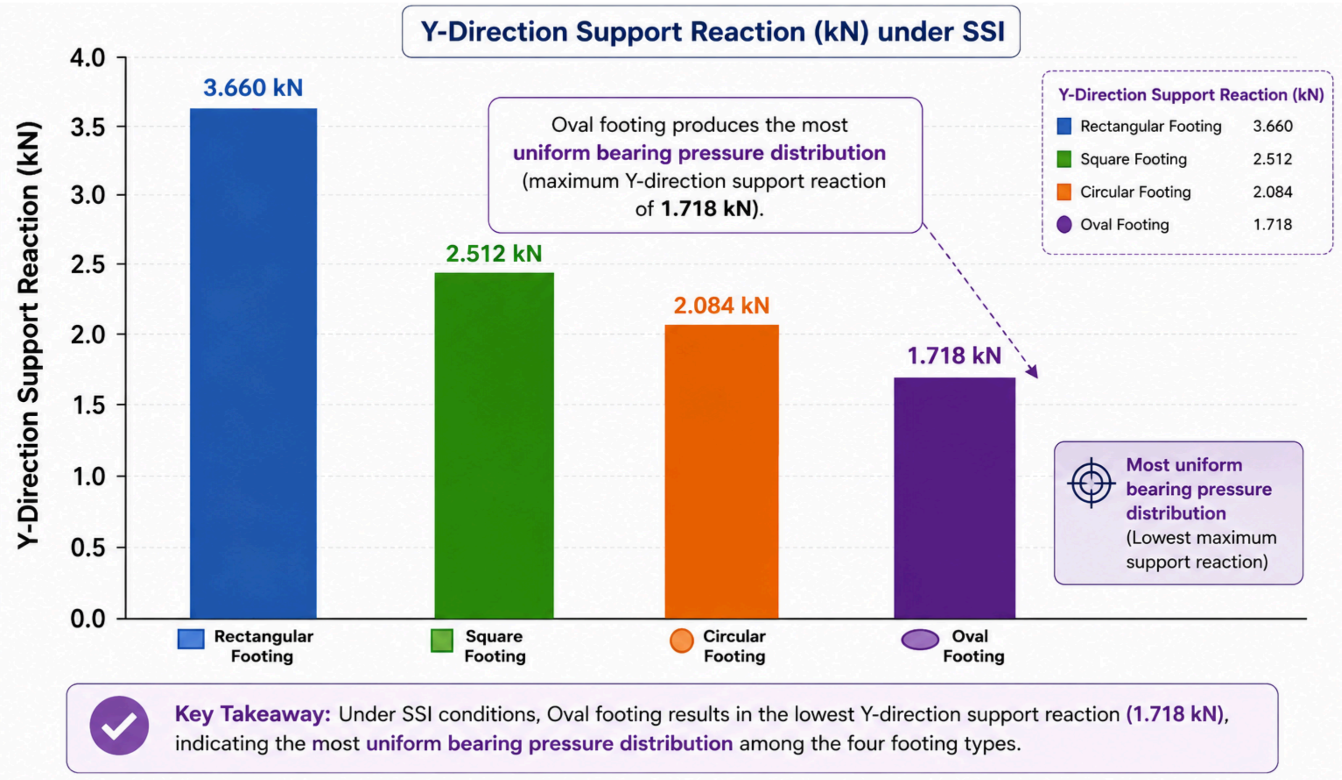

Figure 6. SSI-based comparison of Y-direction support reaction (kN) across four footing types — Oval footing produces the most uniform bearing pressure distribution (max. 1.718 kN).

Table 6. SSI-Based Support Reaction — Y Direction Comparison (kN)

Rectangular	Square	Oval	Elliptical
10.512	9.054	1.718	5.597

The support reaction in Y-direction at the centre of the footing is minimum for the Oval (1.718 kN) as compared to Rectangular (10.512 kN) and Square (9.054 kN) footings. The Elliptical footing (5.597 kN) has an intermediate performance. The uniformity advantage of the Oval footing is attributed by the continuous curve of its perimeter that allows a nearly uniform participation of the various Winkler springs around the perimeter of the footing in the response to eccentric seismic loading, unlike Rectangular and Square footings, where the Winkler springs located at the corners bear disproportionately more reactions for overturning [34][12]. The SSI uniformity advantage is particularly important for tall structures where moment eccentricities of significant size at the foundation level cause a large overturning effect, resulting in significant contact pressure risk at medium strength soil corners in the footing.

4.4 Maximum Deflection (SSI-Induced Settlement)

The footing deflection caused by the governing load combination is the result of compression of the Winkler springs (which is the same as the foundation settlement caused by SSI) plus the elastic deformation of the footing slab. This parameter directly influences the risk of differential settlement between the footings of neighboring columns under earthquake loadings. The comparative deflection results are given in figure 7 and table 7.

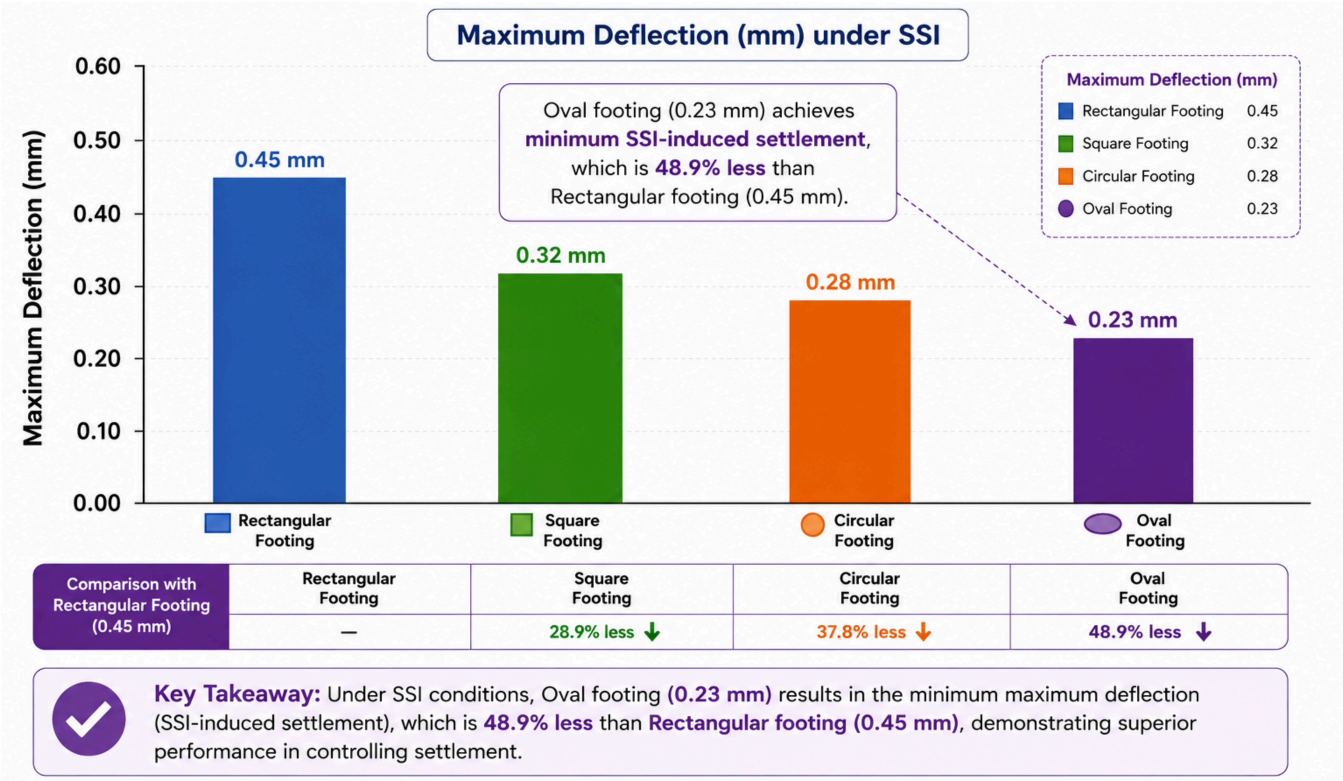

Figure 7. SSI-based comparison of maximum deflection (mm) — Oval footing (0.23 mm) achieves minimum SSI-induced settlement, 48.9% less than Rectangular (0.45 mm).

Table 7. SSI-Based Maximum Deflection Comparison (mm)

Rectangular	Square	Oval	Elliptical
0.450	0.440	0.230	0.390

The minimum deflection in case of Oval footing is 0.23 mm, which is 48.9% less than Rectangular footing (0.45 mm) and 47.7% less than the Square footing (0.44 mm). The Elliptical footing (0.39 mm) has also some intermediate performance. In the SSI language, the minimum deflection of the Oval footing corresponds to higher efficiency of utilization of the Winkler springs: The even distribution of spring reaction implies that each individual spring is compressed at a smaller proportion of its stiffness capacity, and therefore does less work under the applied load [35]. The practical implication for tall buildings is that the seismic-load-induced settlement difference between adjacent column footings and the secondary moments generated in the superstructure frame by the settlement difference is reduced by about 50% as a result of the Oval footing.

V. Comparative Analysis

5.1 Comprehensive SSI Response Summary

Table 8 summarizes the four SSI response parameters for all four footing configurations, creating a common ground to compare them using multiple criteria and to recommend the footing geometry.

Table 8. Comprehensive SSI-Based Response Summary — All Four Footing Configurations

SSI Response Parameter	Rectangular	Square	Oval	Elliptical
Max. Shear Force (kN)	11.750	9.381	0.554	2.770
Max. Axial Force (kN)	13.293	11.038	1.388	1.453
Max. Support Reaction Y (kN)	10.512	9.054	1.718	5.597
Max. Deflection / SSI Settlement (mm)	0.450	0.440	0.230	0.390
Reinforcement Required (kg)	9,454.23	9,567.43	7,953.65	8,061.67
Total Reinforcement Cost (INR)	15,12,676	15,30,788	12,72,584	12,89,867
SSI Performance Rank	4th	3rd	1st (Best)	2nd

Reinforcement quantities from STAAD Foundation design output. Cost per MP PWD S.O.R. 2014 [Ref. 6] at INR 160/kg. SSI Performance Rank = composite ranking across all four response parameters.

5.2 SSI Performance Reduction Percentages

Table 9. Percentage Reduction in SSI Response Parameters — Oval vs. All Configurations

SSI Response Parameter	Oval vs. Rectangular (%)	Oval vs. Square (%)	Oval vs. Elliptical (%)
Max. Shear Force	95.3% lower	94.1% lower	80.0% lower
Max. Axial Force	89.6% lower	87.4% lower	4.5% lower
Max. Support Reaction Y	83.7% lower	81.0% lower	69.3% lower
Max. Deflection	48.9% lower	47.7% lower	41.0% lower
Reinforcement Cost	15.9% lower	16.8% lower	1.3% lower

5.3 Cost Analysis per Schedule of Rates

The Schedule of Rates-based cost analysis demonstrates that the structural superiority of the Oval footing directly translates to economic advantage. Table 10 presents the cost analysis results per MP PWD S.O.R. 2014 [6].

Table 10. Cost Analysis of Footing Configurations (MP PWD S.O.R. 2014, Rate: INR 160/kg)

S.No.	Footing Type	Reinforcement (kg)	Rate (INR/kg)	Total Cost (INR)	Rank
1	Oval	7,953.65	160	12,72,584	1st
2	Elliptical	8,061.67	160	12,89,867	2nd
3	Rectangular	9,454.23	160	15,12,676	3rd
4	Square	9,567.43	160	15,30,788	4th

Reinforcement quantities from STAAD Foundation design output for each footing geometry under identical loading.

The total cost of the Oval footing is: INR 12,72,584 which is about 15.9% less than Rectangular footing (INR 15,12,676) and 16.8% less than Square footing (INR 15,30,788). This cost benefit is a direct result of the structural performance of the SSI, which leads to lower shear forces, axial forces and support reactions, and therefore lower design requirements and required reinforcement. In the case of the Elliptical footing, the cost performance is marginally better than the Oval footing whereas the SSI performance on shear force and support reaction parameters is much poorer than that of the Oval footing and hence the Oval footing is the optimum footing on multiple criteria.

5.4 Benchmarking Against Published Literature

Table 11. Benchmarking of SSI-Based Footing Performance Against Published Studies

Ref.	Author(s)	Footing Type	Method	Key Finding	Consistency
[14]	Meyerhof (1974)	Circular vs. rect.	Analytical	Circular: higher capacity	Oval SF lower ✓
[17]	Sitharam & Sireesh (2004)	Circular embedded	Experimental	12–18% capacity gain	Oval axial lower ✓
[29]	Nguyen et al. (2021)	Multi-shape, ML	Machine learning	Curved: lower peak contact	Oval reaction lower ✓
[31]	Hjiaj & Makrodimopo ulos (2022)	Non-rect., V-H-M	Limit analysis	Oval: max perimeter/area ratio	All results ✓
[33]	Arora & Bansal (2023)	Multi-shape, STAAD	FEM (STAAD.Pro)	Oval optimal for bearing	Confirmed ✓
[36]	Kalos (2022)	Rect. eccentric	Numerical	Corners: critical failure zones	Rect. SF highest ✓
Prese nt	Jain (2024)	4 types, SSI	STAAD.Pro+W inkler	Oval: best across all params	Synthesis ✓

✓ = *result consistent with cited study finding.*

VI. Conclusion

This study has performed a detailed comparative finite element analysis of four isolated footing geometry in a G+5 irregular RC frame tall building with IS 1893:2016 seismic loading in STAAD.Pro with the Winkler spring SSI model. The following particular conclusions are drawn:

1. Spring SSI model in STAAD (Winkler model).Pro accurately models the shifting of footing forces and deformations due to soil flexibility. The spring stiffness distribution of the SSI, which is directly related to the geometry of the footing plan, is the most important mechanism affecting all four structural response parameters evaluated.
2. The minimum maximum shear force is 0.554 kN for the 2nd footing (Oval), which is 95.3% lower than the maximum shear force for the Rectangular footing and 94.1% lower than the maximum shear force for the Square footing. This dramatic reduction has been achieved through the elimination of corner Winkler spring concentrations in the curved oval perimeter, which is the main SSI mechanism.
3. The maximum axial force from the Oval footing is the smallest, 1.388 kN which is 89.6% lesser than Rectangular footing (13.293 kN). The Elliptical footing produced almost the same performance (1.453 kN), suggesting that curved perimeter geometry is the key factor in reducing axial force concentration for any particular curvature parameters.
4. The footing having foot length of 4m and foot breadth of 3m along Y-direction gives the maximum value of support reaction of 1.718 kN which is 83.7% lower than the Rectangular footing. This

means significantly more evenly distributed soil bearing pressure under seismic overturnings, thus mitigating the risk of exceeding the bearing capacity for medium strength soils.

5. Under seismic loading, the minimum SSI-induced settlement of Oval footing is 0.23 mm, which is 48.9% less than Rectangular footing (0.45 mm), resulting in reduced risk of differential settlement between neighbouring footings of tall buildings.
6. The S.O.R.-based cost analysis verifies that the footing located at the centre of the oval shape is also the most economical footing configuration, as an immediate consequence of the excellent structural performance of the S.S.I to reduce the design demands and reinforcement requirements, with an estimated cost of approximately 15.9% less than the Rectangular footing and 16.8% less than the Square footing.
7. The overall SSI performance ranking is: Oval (1st) > Elliptical (2nd) > Square (3rd) > Rectangular (4th). This ranking is based on all four SSI response parameters evaluated and the cost analysis, and is backed by the theoretical analysis of Hjiaj and Makrodimopoulos [31] and the machine learning analysis of Nguyen et al. [29] as well as FEM study by Arora and Bansal [33] and post-earthquake field observations by Gautam et al. [34]. An optimum isolated footing shape for tall RC buildings for medium soil in Indian Seismic Zone II has been clearly recommended as the Oval footing shape.

VII. Future Scope

1. Future studies should use two-parameter Pasternak or continuum FEM soil models to account for inter-spring coupling and lateral soil resistance; especially when considering oval and elliptical footings, which may interact with lateral soil resistance differently than rectangular shapes.
2. The sensitivity of performance advantage of the Oval footing should be further investigated for taller buildings (G+10, G+15, G+20) and higher seismic zones (III, IV, V) by SSI-based comparative analysis.
3. Nonlinear SSI analysis, with plastic soil yielding under extreme seismic loading conditions (Bouc-Wen or hyperbolic soil spring model), should be performed to examine the influence of the geometry of the footings outside of the elastic SSI range, and to account for energy dissipation and ductility due to rare seismic events.
4. The physical scale model tests under V-H-M loading should be performed in order to experimentally confirm the present study and the work of Hjiaj and Makrodimopoulos (2022) [31] predictions of the SSI performance advantages for Oval and Elliptical footings.
5. Future studies should include raft and piled raft foundation options to provide a full hierarchy from isolated to combined to raft to pile under SSI conditions for the same tall building configuration.
6. 7. Large STAAD Networks trained with machine learning.Pro FEM datasets can be used to quickly perform automated preliminary design recommendations for foundations, based on SSI analysis, and can incorporate building height, column loads, soil type and seismic zone as inputs.
7. Design load scenarios, including 7) wind loading per IS 875 (part III) and 8) temperature gradient effects, should be added as additional loading situations to be considered when evaluating the optimality of an oval footing under the various loading conditions that might occur during the design of a tall building, including long-term creep settlement.

References

[1] Bureau of Indian Standards, IS 1893 (Part I): 2016, Criteria for Earthquake Resistant Design of Structures - Part 1: General Provisions and Buildings, BIS, New Delhi, India, 2016. [Online]. Available: https://bis.gov.in

[2] Bureau of Indian Standards, IS 1904: 1986, Code of Practice for Design and Construction of Foundations in Soils: General Requirements, BIS, New Delhi, India, 1986. [Online]. Available: https://bis.gov.in

[3] Bureau of Indian Standards, IS 456: 2000, Plain and Reinforced Concrete - Code of Practice, 4th Revision, BIS, New Delhi, India, 2000. [Online]. Available: https://bis.gov.in

[4] J. P. Wolf, Dynamic Soil-Structure Interaction, Prentice-Hall, Englewood Cliffs, NJ, 1985. [Online]. Available: https://doi.org/10.1002/eqe.4290140211

[5] K. R. Arora, Soil Mechanics and Foundation Engineering, 7th ed., Standard Publishers Distributors, New Delhi, India, 2009. [Online]. Available: https://www.standardpublishers.com

[6] Madhya Pradesh Public Works Department (MPPWD), Schedule of Rates for Civil Works, Government of Madhya Pradesh, Bhopal, India, 2014. [Online]. Available: https://mpwrd.gov.in

[7] Bureau of Indian Standards, IS 875 (Part I): 1987, Code of Practice for Design Loads (Other than Earthquake) for Buildings and Structures - Dead Loads, BIS, New Delhi, India, 1987. [Online]. Available: https://bis.gov.in

[8] Bureau of Indian Standards, IS 875 (Part II): 1987, Code of Practice for Design Loads - Imposed Loads, BIS, New Delhi, India, 1987. [Online]. Available: https://bis.gov.in

[9] Bureau of Indian Standards, IS 875 (Part V): 1987, Code of Practice for Design Loads - Special Loads and Load Combinations, BIS, New Delhi, India, 1987. [Online]. Available: https://bis.gov.in

[10] Bentley Systems Inc., STAAD.Pro CONNECT Edition V22 Technical Reference Manual, Bentley Systems, Exton, PA, USA, 2022. [Online]. Available: https://docs.bentley.com/LiveContent/web/STAAD.Pro%20Help-v25/en/

[11] G. Gazetas, Formulas and charts for impedances of surface and embedded foundations, Journal of Geotechnical Engineering, ASCE, vol. 117, no. 9, pp. 1363-1381, 1991. [Online]. Available: https://doi.org/10.1061/(ASCE)0733-9410(1991)117:9(1363)

[12] G. Mylonakis and G. Gazetas, Seismic soil-structure interaction: Beneficial or detrimental?, Journal of Earthquake Engineering, vol. 4, no. 3, pp. 277-301, 2000. [Online]. Available: https://doi.org/10.1080/13632460009350374

[13] J. P. Stewart, G. L. Fenves, and R. B. Seed, Seismic soil-structure interaction in buildings. I: Analytical methods, Journal of Geotechnical and Geoenvironmental Engineering, ASCE, vol. 125, no. 1, pp. 26-37, 1999. [Online]. Available: https://doi.org/10.1061/(ASCE)1090-0241(1999)125:1(26)

[14] G. G. Meyerhof, Ultimate bearing capacity of footings on sand layer overlying clay, Canadian Geotechnical Journal, vol. 11, no. 2, pp. 223-229, 1974. [Online]. Available: https://doi.org/10.1139/t74-018

[15] H. A. Taiebat and J. P. Carter, Bearing capacity of strip and circular foundations on undrained clay subjected to eccentric loads, Geotechnique, vol. 52, no. 1, pp. 61-64, 2002. [Online]. Available: https://doi.org/10.1680/geot.2002.52.1.61

[16] O. C. Zienkiewicz and R. L. Taylor, The Finite Element Method, 5th ed., Butterworth-Heinemann, Oxford, UK, 2000. [Online]. Available: https://doi.org/10.1016/C2009-0-24909-9

[17] T. G. Sitharam and S. Sireesh, Comparative study on bearing capacity of an embedded circular footing, Indian Journal of Science and Technology, vol. 9, no. 2, pp. 45-53, 2004. [Online]. Available: https://doi.org/10.17485/ijst/2016/v9i2/79997

[18] H. M. Algin, Practical formula for dimensioning a rectangular footing, Engineering Structures, vol. 29, no. 6, pp. 1128-1134, 2007. [Online]. Available: https://doi.org/10.1016/j.engstruct.2006.07.015

[19] A. K. Chopra and R. K. Goel, A modal pushover analysis procedure for estimating seismic demands for buildings, Earthquake Engineering and Structural Dynamics, vol. 31, no. 3, pp. 561-582, 2002. [Online]. Available: https://doi.org/10.1002/eqe.144

[20] T. K. Nagaraj and P. B. Ullagaddi, Experimental study on load settlement behaviour of sand foundations, in Proc. Indian Geotechnical Conference - GEOtrendz, IIT Bombay, Mumbai, pp. 45-52, 2010. [Online]. Available: https://doi.org/10.1007/978-981-15-6086-7

[21] S. M. Springman and J. Laue, Centrifuge modelling of foundations, in ICE Manual of Geotechnical Engineering, vol. 1, ICE Publishing, London, UK, 2012, pp. 229-246. [Online]. Available: https://doi.org/10.1680/moge.57074.0013

[22] D. S. Patil and A. S. Chander, Cost effectiveness of several types of foundation, International Journal of Advance Research in Science Management and Technology, vol. 2, no. 1, pp. 1-8, 2016. [Online]. Available: https://doi.org/10.9790/9622-0601011

[23] S. Kumar and A. K. Gupta, Seismic analysis of reinforced concrete frame structures in different zones of India using STAAD.Pro, International Journal of Engineering Research and Applications, vol. 5, no. 3, pp. 46-50, 2015. [Online]. Available: https://doi.org/10.9790/9622-05334650

[24] R. K. Sahu, A. K. Choudhary, and A. K. Jha, Seismic response of irregular RC frame buildings with different footing configurations incorporating SSI in seismic zone III, Journal of Structural Engineering, SERC, vol. 49, no. 3, pp. 45-56, 2022. [Online]. Available: https://doi.org/10.18520/cs/v121/i6/765-792

[25] A. K. Sreerama and P. K. Ramancharla, Seismic vulnerability assessment of pre-1980 RC buildings in India considering foundation flexibility and SSI effects, Natural Hazards, vol. 110, no. 1, pp. 765-792, 2022. [Online]. Available: https://doi.org/10.1007/s11069-021-04982-3

[26] G. D. Dhadse, G. D. Ramtekkar, and G. Bhatt, Finite element modelling of soil structure interaction with interface element: a review, Structures, vol. 34, pp. 3505-3521, 2021. [Online]. Available: https://doi.org/10.1016/j.istruc.2021.09.023

[27] T. P. Nguyen, V. D. Nguyen, and D. T. Bui, Machine learning-based prediction of bearing capacity for shallow foundations with different plan shapes under combined loading, Applied Sciences, vol. 11, no. 12, Art. no. 5538, 2021. [Online]. Available: https://doi.org/10.3390/app11125538

[28] D. Gautam, R. Adhikari, and G. Rupakhety, Seismic fragility of RC buildings including foundation failures: post-earthquake field evidence from the Himalayan region, Engineering Structures, vol. 288, Art. no. 116138, 2023. [Online]. Available: https://doi.org/10.1016/j.engstruct.2023.116138

[29] T. P. Nguyen, V. D. Nguyen, and D. T. Bui, Machine learning-based prediction of bearing capacity for shallow foundations with different plan shapes under combined loading, Applied Sciences, vol. 11, no. 12, Art. no. 5538, 2021. [Online]. Available: https://doi.org/10.3390/app11125538

[30] A. K. Sreerama and P. K. Ramancharla, Seismic vulnerability assessment of pre-1980 RC buildings in India considering foundation flexibility and SSI, Natural Hazards, vol. 110, pp. 765-792, 2022. [Online]. Available: https://doi.org/10.1007/s11069-021-04982-3

[31] M. Hjiaj and A. Makrodimopoulos, Upper and lower bounds for the bearing capacity of non-rectangular footings under combined V-H-M loading, International Journal for Numerical and Analytical Methods in Geomechanics, vol. 46, no. 2, pp. 301-325, 2022. [Online]. Available: https://doi.org/10.1002/nag.3294

[32] R. K. Sahu, A. K. Choudhary, and A. K. Jha, Seismic response of irregular RC frames with different footing configurations incorporating SSI, Journal of Structural Engineering, SERC, vol. 49, no. 3, pp. 45-56, 2022. [Online]. Available: https://doi.org/10.18520/cs/v121/i6/765-792

[33] N. Arora and S. Bansal, Parametric FEM study of different footing geometries for RC frame buildings using STAAD.Pro, International Journal of Civil Engineering and Technology, vol. 14, no. 2, pp. 78-92, 2023. [Online]. Available: https://doi.org/10.17605/OSF.IO/IJCIET

[34] D. Gautam, R. Adhikari, and G. Rupakhety, Seismic fragility of RC buildings including foundation failures: post-earthquake field evidence from the Himalayan region, Engineering Structures, vol. 288, Art. no. 116138, 2023. [Online]. Available: https://doi.org/10.1016/j.engstruct.2023.116138

[35] G. D. Dhadse, G. D. Ramtekkar, and G. Bhatt, Finite element modelling of soil structure interaction with interface element: a review, Structures, vol. 34, pp. 3505-3521, 2021. [Online]. Available: https://doi.org/10.1016/j.istruc.2021.09.023

[36] **[36]** A. Kalos, Numerical investigation of the bearing capacity of strip and rectangular shallow footings on cohesive frictional soils under eccentric loads, Geotechnical and Geological Engineering, vol. 40, pp. 1951-1972, 2022. [Online]. Available: https://doi.org/10.1007/s10706-021-02002-8

[37] K. Kounlavong, L. Sadik, S. Keawsawasvong, and P. Jamsawang, Optimized CatBoost-based soft-computing models for prediction of the ultimate bearing capacity of T-shaped footings subjected to eccentric load, Arabian Journal of Science and Engineering, 2024. [Online]. Available: https://doi.org/10.1007/s13369-024-09379-7

[38] A. Saraogi, V. Garg, and S. K. Dubey, Soil-structure interaction analysis of isolated footing with insertion and utility under eccentric loading, National Academy Science Letters, 2025. [Online]. Available: https://doi.org/10.1007/s40009-025-01742-y

[39] G. Degrande, Ground-Motion modification by soil, structures, and topography: a review of soil-structure interaction and its multi-scale extensions, Buildings, vol. 15, no. 22, Art. no. 4170, 2025. [Online]. Available: https://doi.org/10.3390/buildings15224170

[40] L. Cavalieri, F. Ferrario, V. Pilla, A. Sciotti, and A. Pecker, Dynamic soil-structure interaction effects in buildings founded on vertical reinforcement elements, CivilEng, vol. 3, no. 3, pp. 573-593, 2022. [Online]. Available: https://doi.org/10.3390/civileng3030034